Precambrian Research 183 (2010) 805–816

Contents lists available at ScienceDirect

Precambrian Research

journal homepage: www.elsevier.com/locate/precamres

Tracing the 850-Ma continental flood basalts from a piece of subducted continental crust in the North Qaidam UHPM belt, NW China

Shuguang Song[a,*], Li Su[b], Xian-hua Li[c], Guibing Zhang[a], Yaoling Niu[d], Lifei Zhang[a]

[a] MOE Key Laboratory of Orogenic Belts and Crustal Evolution, School of Earth and Space Sciences, Peking University, #5 Yiheyuan Road, Haidian, Beijing 100871, China
[b] Geological Lab Center, China University of Geosciences, Beijing 100083, China
[c] State Key Laboratory of Lithospheric Evolution, Institute of Geology and Geophysics, Chinese Academy of Sciences, Beijing 100029, China
[d] Department of Earth Sciences, Durham University, Durham DH1 3LE, UK

ARTICLE INFO

Article history:
Received 12 April 2010
Received in revised form 9 September 2010
Accepted 22 September 2010

Keywords:
Eclogite blocks
CFB
Zircon U–Pb age
850 Ma mantle plume
North Qaidam UHP belt
Continental subduction

ABSTRACT

A Paleozoic ultrahigh-pressure metamorphic (UHPM) belt extends along the northern margin of the Qaidam Basin, North Tibetan Plateau. Eclogites in the Yuka eclogite terrane, northwest part of this UHPM belt, occur as blocks or layers of varying size intercalated with granitic and pelitic gneisses. These eclogites have protoliths geochemically similar to enriched-type mid-ocean ridge basalts (E-MORB) and oceanic island basalts (OIB). On the basis of Ti/Y ratios, they can be divided into low-Ti and high-Ti groups. The low-Ti group (LTG) eclogites exhibit relatively low TiO_2 (most <2.5 wt%) and Ti/Y (<500) but comparatively high Mg# (48–55), whereas the high-Ti group (HTG) eclogites have high TiO_2 (most >2.5 wt%) and Ti/Y (>500) but lower Mg# (46–52). Zircons from two eclogite samples gave a magmatic crystallization (protolith) age of ~850 Ma and a UHPM age of ~433 Ma. The occurrence, geochemical features and age data of the Yuka eclogites suggest that their protoliths are segments of continental flood basalts (CFBs) with a mantle plume origin, similar to most typical CFBs. Our observation, together with the tectonic history and regional geologic context, lend support for the large scale onset of mantle plume within the Rodinia supercontinent at ~850 Ma. The Qaidam block is probably one of the fragments of the Rodinia supercontinent with a volcanic-rifted passive margin. The latter may have been dragged to mantle depths by its subducting leading edge of the oceanic lithosphere in the Early Paleozoic.

1. Introduction

Continental flood basalts (CFBs) with the geochemistry similar to that of ocean island basalts (OIB) may be of mantle plume origin, and represent volumetrically significant and rapidly emplaced melts produced by decompression melting of rising mantle plume heads (e.g., White and McKenzie, 1989; Richards et al., 1989; Campbell and Griffiths, 1990; Coffin and Eldholm, 1994; Puffer, 2001). The ~830–750 Ma Neoprotozoic continental intraplate magmatism widespread in Australia, Laurentia and South China has been attributed to a long-lived mantle plume or superplume that may have triggered the breakup of the supercontinent Rodinia (e.g., Heaman et al., 1992; Zhao et al., 1994; Park et al., 1995; Li et al., 1999, 2002, 2003, 2006, 2008a, 2010; Frimmel et al., 2001; Shellnutt et al., 2004; Wang et al., 2007, 2008).

The onset time of the long-lived Neoproterozoic plume (or superplume) activity, however, remains poorly constrained. It is generally thought that Rodinia was assembled through worldwide orogenic events between 1300 Ma and 900 Ma and started to break up at ~825 Ma (e.g., Li et al., 2008a and references therein). Between the time interval from 900 Mato 830 Ma, little geological record is available within Rodinia, and only a small number of 870–850 Ma intrusions such as those in South China, Africa, the Scandinavian Caledonides and the Scottish promontory of Laurentia have been reported (Li et al., 2003, 2010; Paulsson and Andreasson, 2002; Dalziel and Soper, 2001), which were interpreted as representing the beginning of the break-up of Rodinia. However, this interpretation may be questionable as the petrogenesis of these intrusions is unclear and could very well record post-orogenic magmatism associated with the Grenvill orogeny or other intraplate (non-orogenic) magmatism. Consequently, Li et al. (2008a) concluded that a widespread plume activity did not occur until ~825 Ma.

The North Qaidam UHPM belt extends in NW-direction between the Qaidam block and Qilian block on the northern Tibetan Plateau, NW China (Fig. 1a). It is a type continental subduction zone with exhumed rocks dominated by granitic and pelitic gneisses with lesser amounts of eclogite and garnet peridotite (Yang et al., 1998, 2001, 2002, 2006; Song et al., 2003a,b, 2005, 2006, 2009a,b; Zhang et al., 2005, 2008b; Mattinson et al., 2006, 2007). Reliable zircon U–Pb ages indicate that the UHP metamorphism and subsequent

* Corresponding author. Tel.: +86 10 62767729; fax: +86 10 62767729.
E-mail address: sgsong@pku.edu.cn (S. Song).

0301-9268/$ – see front matter © 2010 Elsevier B.V. All rights reserved.
doi:10.1016/j.precamres.2010.09.008

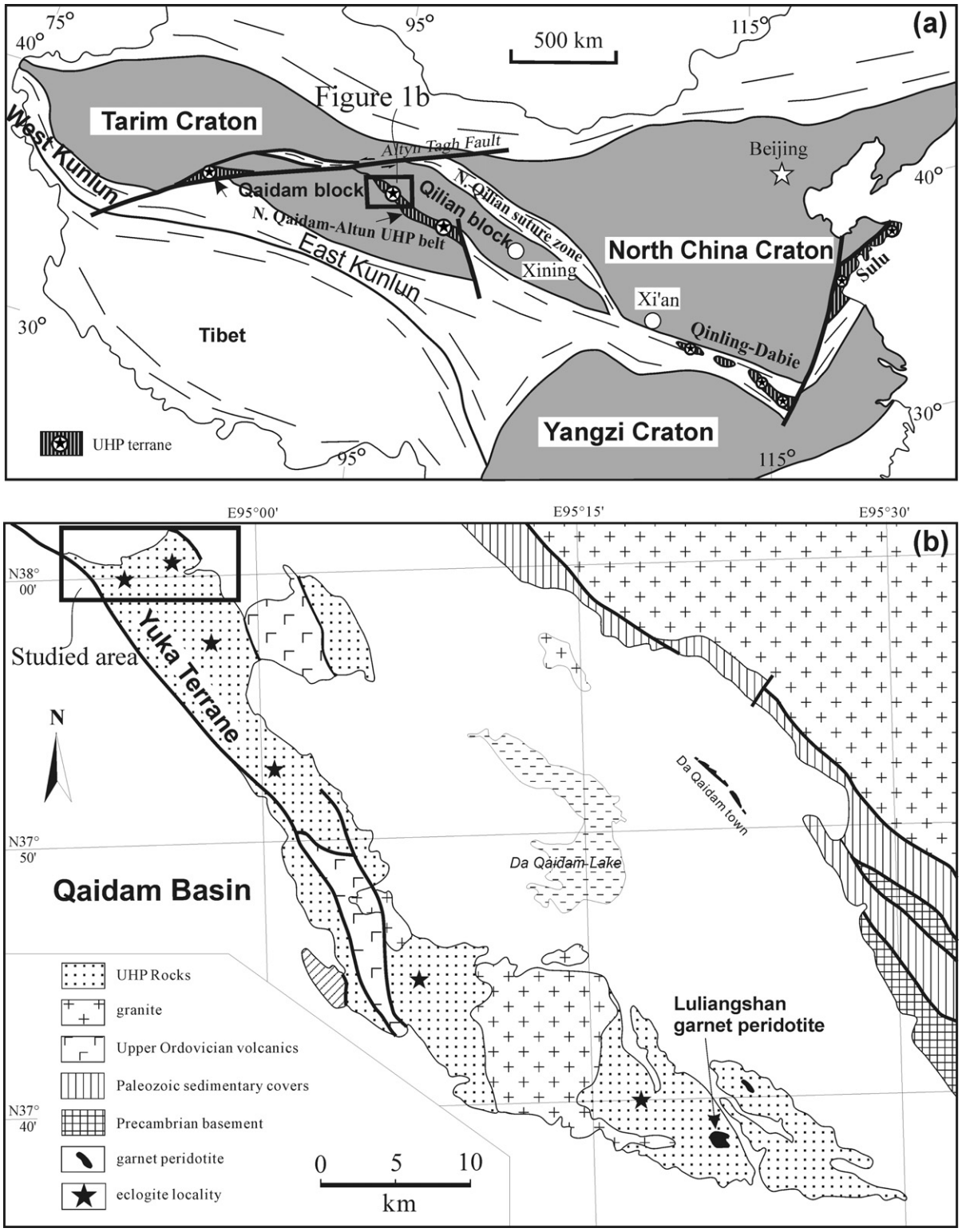

Fig. 1. (a) Schematic maps showing major tectonic units of China (after Song et al., 2006). (b) Geological map of the Yuka eclogite-bearing terrane.

exhumation occurred from ~460 Ma to 400 Ma (Song et al., 2003a, 2005, 2006; Mattinson et al., 2006, 2009; Zhang et al., 2008b,a; Chen et al., 2009). On the basis of the geochemistry and age data, Song et al. (2006) demonstrated that this UHP belt had undergone an evolution history from oceanic subduction at ~460–440 Ma, to continental subduction at ~430–420 Ma, and to exhumation at ~400 Ma. Recognition of the UHP metamorphosed ophiolitic sequences with protolith ages of ~550–500 Ma in the Dulan terrane at the east end of this UHPM belt (Zhang et al., 2008a, 2009a,b; Song et al., 2009b) supports the above interpretations.

In this paper, we present elemental and Nd isotopic data and SIMS zircon U–Pb ages for the Yuka eclogites hosted in the granitic and pelitic gneisses in the northwest part of the UHPM belt. We show that the protoliths of the Yuka eclogite blocks have geo-

chemical characteristics resembling those of OIB or CFB with a magmatic age of ~850 Ma. We interpret the protoliths, along with other geological observations, as representing fragments of a suite of continental flood basalts, whose geochemistry and magmatic age of ~850 Ma favors a mantle plume origin with the supposed plume head probably underlain Rodinia in the Neoproterozoic time. The Yuka eclogite protoliths were probably emplaced at a volcanic-rifted passive continental margin associated with the break-up of Rodinia.

2. Geological settings

The North Qaidam UHPM belt is located at the northern margin of the Tibet Plateau. It extends approximately 400 km and is offset by the Altyn Tagh Fault, a large sinistral strike-slip fault system in western China (Fig. 1a). To the south is the Qaidam block, a Mesozoic intercontinental basin with a Precambrian basement that remains poorly studied. To the north is the Qilian block with a Precambrian basement similar to the Yangtze Craton (Wan et al., 2001; Song et al., 2006; Chen et al., 2009). Further to the north is the North Qilian Early Paleozoic subduction-zone complexes with ophiolite, lawsonite-bearing eclogite and carpholite-bearing metapelite, which is interpreted to be the suture zone between the North and South China Cratons (i.e., Song et al., 2009a and references therein).

The North Qaidam UHPM belt consists mainly of a typical *continental-type* subduction zone rock assemblage of granitic and pelitic gneisses intercalated with blocks of eclogite and ultramafic rocks. From northwest to southeast, there are three discrete terranes along the UHPM belt, i.e., the Yuka-Luliangshan, the Xitieshan and Dulan terranes. The presence of coesite and diamond inclusions in zircons and garnets suggests UHPM conditions, similar to continental-type UHPM terranes elsewhere in the world (Yang et al., 2001, 2002; Song et al., 2003a, 2005). In the Dulan UHPM terrane, UHP metamorphosed ophiolite sequences, including serpentinized harzburgite, banded ultramafic to mafic cumulate (kyanite–eclogite) and massive eclogite with N- to E-MORB affinities, suggest a former oceanic subduction prior to the continental subduction (Song et al., 2003b, 2009b; Zhang et al., 2008a). The age data indicate that the ophiolite was formed at ~500–550 Ma and metamorphosed at HP–UHP conditions at ~460–420 Ma. The garnet peridotite in the Luliangshan region (see Fig. 1b for its locality), which is interpreted as layered ultramafic complex, has been subducted to depths greater than 200 km (Song et al., 2004, 2005, 2007). The eclogite in the Yuka terrane was first reported by Yang et al. (1998) and further studied by Zhang et al. (2005) and Chen et al. (2009). Recently, Zhang et al. (2009a,b) reported UHP minerals (e.g., coesite) from the Yuka eclogite, which is consistent with the calculated metamorphic *P*–*T* conditions of *P* = 2.8–3.2 GPa and *T* = 650–700 °C. In situ LA-ICPMS zircon U–Th–Pb dating yielded metamorphic ages of 431 ± 4 to 436 ± 3 for eclogite and 431 ± 3 to 432 ± 19 Ma for the hosting gneisses (Chen et al., 2009). Inherited cores in zircons give ages of ~750–800 Ma (Zhang et al., 2008b; Chen et al., 2009).

3. Field occurrence and petrography

3.1. Gneisses

There are two types of felsic gneisses, pelitic paragneiss (PG) and granitic orthogneiss (GG). The former (PG) is volumetrically minor, and is mostly interbedded with the eclogites (Fig. 2a and b). It contains a metamorphic assemblage of garnet + muscovite + quartz + plagioclase ± kyanite ± allanite with varying modal contents between samples. The granitic orthogneiss occupies ~70 vol.% of the Yuka eclogite–gneiss terrane. The granitic gneisses are white to pale grey and show medium- to coarse-grained granoblastic texture with strong foliation. They consist of K-feldspar, plagioclase, quartz, muscovite, and tourmaline with garnet in some samples. Zircon U–Pb dating give ~950 Ma (Lu, 2002; Chen et al., 2009).

3.2. Eclogite

Eclogites occur as lens-like blocks of varying size, layers and boudinaged dykes within both granitic and pelitic gneisses (Fig. 2). Some eclogite layers extend for more than 1 km in length (Fig. 2b). Most eclogites are fresh, show a medium- to coarse-grained granular texture and have a typical mineral assemblage of garnet, omphacite, rutile and phengite (Fig. 3a–c) with subsequent amphibole overprinting. Zircons are seen as euhedral crystals in the matrix (Fig. 3d) and as small (<50 μm) rounded inclusions in garnet.

4. Analytical methods and data

All the samples are fresh cuttings away from late veinlets (metamorphic or magmatic impregnation, etc.) with pen marks, saw marks, sticker residues, and other suspicious surface contaminants ground off before thorough cleaning. The samples were then reduced to 1–2 cm size chips using a percussion mill with minimal powder production. These rock pieces were then ultrasonically cleaned in Milli-Q water, dried, and powdered in a thoroughly cleaned agate mill in the clean laboratory at the Langfang Regional Geological Survey, China.

Bulk-rock major element oxides (SiO_2, TiO_2, Al_2O_3, FeO, MnO, MgO, CaO, Na_2O, K_2O, and P_2O_5) were analyzed using a Leeman Prodigy inductively coupled plasma-optical emission spectroscopy (ICP-OES) system with high dispersion Echelle optics at China University of Geosciences, Beijing (CUGB; Table 1, Supplementary data). Precisions (1σ) for most elements based on rock standards BCR-1, AGV-2 (US Geological Survey (USGS)) and GSR-3 (national geological standard reference materials (SRM) of China) are better than 1% with the exception of TiO_2 (~1.5%) and P_2O_5 (~2.0%). Loss on ignition (LOI) was determined by placing 1 g of samples in the furnace at 1000 °C for several hours before being cooled in a desiccator and reweighed.

Whole-rock trace element analyses for the Yuka eclogites (Table 1, Supplementary data) were performed on an Agilent-7500a inductively coupled plasma mass spectrometry (ICP-MS) at CUGB. Fifty mg powder of each sample was dissolved in equal mixture of subboiling distilled HF and HNO_3 with a Teflon digesting vessel on a hot-plate for 24 h using high-pressure bombs to ensure complete digestion/dissolution. This procedure was repeated using smaller amounts of acids for a further 12 h. After digestion, the sample was evaporated to incipient dryness, refluxed with 6 N HNO_3, and heated again to incipient dryness. The sample was then dissolved in 2 ml of 3 N HNO_3 and diluted with Milli-Q water (18 MΩ) to a final dilution factor of 2000. Two USGS rock reference materials BCR-1 and BHVO-1 were used to monitor the analytical accuracy and precision. Analytical accuracy, as indicated by relative difference (RE) between measured and recommended values is better than 5% for most elements, ranging between 10% and 13% for Cu, Sc, Nb, Er, Th, and U, and between 10% and 15% for Ta, Tm, and Gd.

Sm–Nd isotopic compositions of representative samples (Table 2, Supplementary data) were determined using a Micromass Isoprobe multi-collector ICP-MS (MC-ICP-MS) in the Guangzhou Institute of Geochemistry following Li et al. (2004). Measured $^{143}Nd/^{144}Nd$ ratios were normalized to $^{146}Nd/^{144}Nd = 0.7219$, and the reported $^{143}Nd/^{144}Nd$ ratios were further adjusted relative to the Shin Etsu JNdi-1 standard of 0.512115. Initial

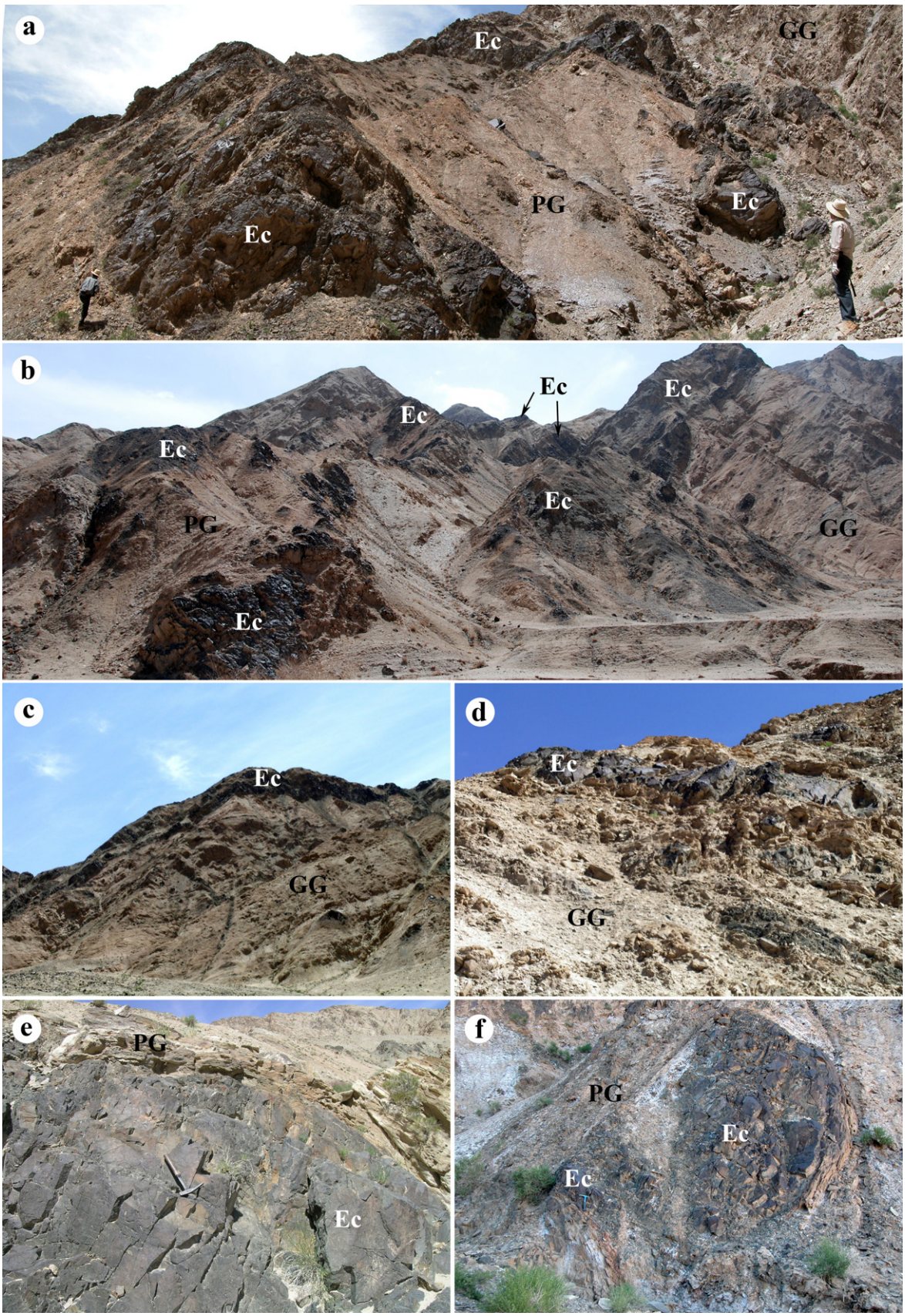

Fig. 2. Photographs showing occurrence of the Yuka eclogite blocks. (a) Eclogite layers interbedded with paragneisses. (b) Thick eclogite layers that extend about 1 km; some are retrograde into garnet-amphibolite. (c) Eclogite layer covering the granitic gneiss. (d) Dyke-like eclogite blocks within the granitic gneiss. (e) and (f) Lentoid eclogite blocks within the pelitic gneiss.

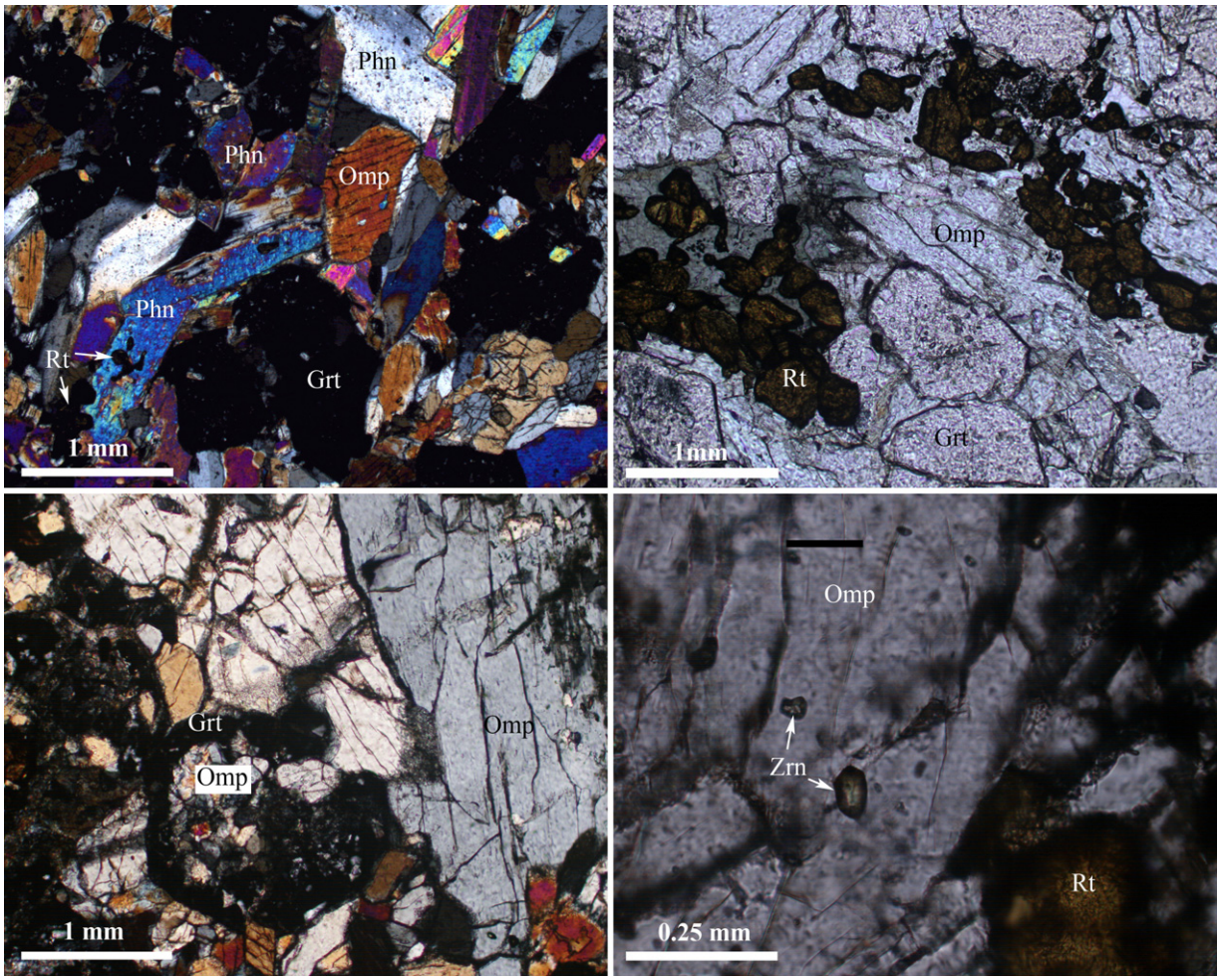

Fig. 3. Photomicrographs showing texture and mineral assemblage of the Yuka eclogite. (a) Mineral assemblage garnet (Grt), omphacite (Omp), phengite (Phn) and rutile (Rt) of the HTG eclogite (2C87). (b) Rutile aggregate in the HTG eclogites (2C87). (c) Skeletal Grt and Omp in the LTG eclogite (2C125). (d) Euhedral zircon in the HTG eclogite (2C87).

$^{143}Nd/^{144}Nd$ ratios and corresponding $\varepsilon_{Nd}(t)$ values were calculated on the basis of present-day reference values for chondritic uniform reservoir (CHUR): $(^{143}Nd/^{144}Nd)_{CHUR} = 0.512638$ and $(^{147}Sm/^{144}Nd)_{CHUR} = 0.1967$.

Two eclogite samples (2C87 and 4Y04) from the Yuka terrane were chosen for zircon U–Pb geochronological study. They were crushed and sieved to <300 μm. Zircon grains were separated using standard density and magnetic separation techniques, and finally hand-picked under a binocular microscope. They were then embedded in 25 mm epoxy discs and polished down to half-sections. The internal structure of zircon grains was examined using a cathodoluminescent (CL) spectrometer (Garton Mono CL3+) equipped on a Quanta 200F ESEM with 45-s scanning time at conditions of 15 kV and 120 nA at Peking University.

Measurements of U, Th and Pb were conducted using SHRIMP II at Australian National University (ANU) (sample 4Y04) and the Cameca IMS-1280 ion microprobe at the Institute of Geology and Geophysics, Chinese Academy of Sciences in Beijing (sample 2C87). Analytical procedures of SHRIMP II have been described in Rubatto et al. (1998). Data given in Supplementary data Table 3 have 1σ errors. Operation conditions and data reduction procedures for Cameca IMS-1280 analyses have been described in Li et al. (2009). U–Th–Pb ratios and absolute abundances were determined relative to the zircon standard 91500 (Wiedenbeck et al., 1995), which was analyzed repeatedly between samples. The mass resolution used to measure Pb/Pb and Pb/U isotopic ratios was 5400 during the analysis. Measured compositions were corrected for common Pb using non-radiogenic ^{204}Pb. Corrections are sufficiently small and are insensitive to the choice of common Pb composition. An average of present-day crustal composition (Stacey and Kramers, 1975) is used for the common Pb assuming that the common Pb is largely from surface contamination introduced during sample preparation. The data are summarized in Supplementary data Table 4. Uncertainties on individual analyses are reported using 1σ errors, and weighted mean ages for pooled $^{206}Pb/^{238}U$ results are quoted at a 95% confidence level.

5. Data interpretation

5.1. Classification of protoliths of the Yuka eclogite

We use Ti/Y ratio to finger-print the protoliths of the eclogites because this ratio is generally less sensitive to fractional crystallization of basaltic magmas (e.g., Peate et al., 1992; Xu et al., 2001) and because both Ti and Y are relatively immobile during metamorphism. The 18 analyzed samples can be divided into two major groups: high-Ti group (HTG, Ti/Y > 500) and low-Ti group (LTG, Ti/Y < 500). Fig. 4 shows that the Ti/Y ratios of the Yuka eclogites are correlated with Mg# (indicator of differentiation) and Sm/Yb (degree of HREE fractionation, reflecting the effect of source variation or varying contributions of melt from the garnet peridotite facies). In general, the LTG samples have higher Mg# and lower

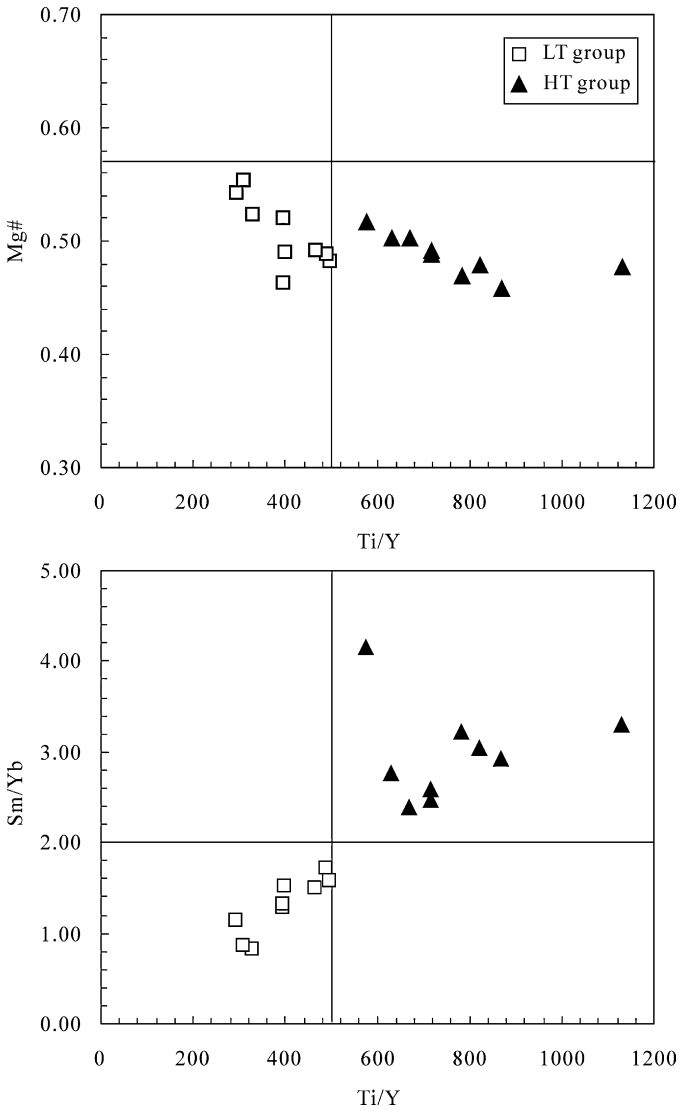

Fig. 4. Diagram showing variation of Mg# and Sm/Yb against Ti/Y for the Yuka eclogites.

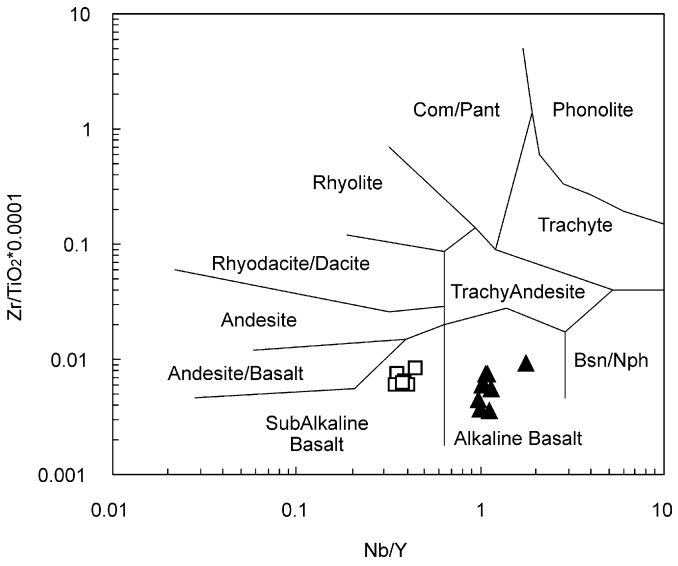

Fig. 5. Classification using Nb/Y vs Zr/Ti diagram for the Yuka eclogites.

Sm/Yb ratio compared to most HTG samples. In Nb/Y vs. Zr/Ti diagram (Winchester and Floyd, 1977), all HTG samples plot in the alkaline basalt field, whereas the LTG samples are in the sub-alkaline basalt field (Fig. 5).

5.2. Whole-rock major elements

All Yuka eclogite samples display a relative narrow compositional variation in SiO_2 (43.33–49.47 wt%), total Fe_2O_3 (Fe_2O_3t, 12.56–16.34 wt%), MgO (5.3–7.3 wt%) and Mg-number (Mg# = 0.55–0.46), but a wide range in $K_2O + Na_2O$ (2.64–4.83 wt%) and TiO_2 (1.38–4.04 wt%). Both alkali and TiO_2 show negative correlations with SiO_2. The low-Ti group exhibits low Ti/Y (<500) with TiO_2 <2.5 wt% in most samples (only one sample is 2.6), and the high-Ti group samples (Ti/Y > 500) have high TiO_2 (most >2.5 wt% except sample 4Y27).

5.3. Trace elements

The HTG and LTG eclogite samples are distinct in terms of minor and trace element compositions. As expected, the HTG samples have higher HFSE (high-field strength elements) than the LTG. On chondrite-normalized REE and primitive-mantle normalized trace element diagrams (Fig. 6), the HTG samples have higher abundances of REEs (ΣREE = 122–199 ppm) and greater light REE enrichment ($[La/Yb]_N$ = 5.22–17.23) than the LTG samples (ΣREE = 48–106 ppm; $[La/Yb]_N$ = 1.56–2.95). Also, the LTG samples show a large variation in Rb and Ba, and are strongly depleted related to Th in some samples. All LTG samples have a positive U anomaly. Sr is also variable in the LTG samples with both positive and negative anomalies. On the other hand, most HTG samples show smooth or a negative Sr anomaly related to Pr and Nd (except 4Y27). In general, except for variable LILEs (e.g., Rb, Ba, U and Sr) which could be caused by their mobility during seafloor or subduction-zone metamorphism, the HTG samples show "immobile" trace elements characteristics resembling the present-day ocean island basalts (OIB), whereas the LTG samples resemble the present-day enriched type mid-ocean ridge basalts (E-MORB) or transitional type.

5.4. Nd-isotope

Nd isotopic data are given in Supplementary data Table 2. The initial isotopic ratios were corrected to 847 Ma (see below). The Yuka eclogites display a wide range of $^{143}Nd/^{144}Nd$ values from 0.512160 to 0.512699 with $\varepsilon_{Nd}(t = 847\ Ma)$ varying from +5.07 to −7.96, more enriched than MORB and most OIB.

5.5. Zircon U–Pb ages

Two samples (2C87 and 4Y04) used for zircon U–Pb dating are fresh eclogites with mineral assemblage of garnet, omphacite (Jd_{30-35}), phengite (Si = 3.35–3.4 p.f.u.), rutile, minor amphibole, apatite and zircon (Fig. 3). About 300 zircon grains were recovered from each sample of ~5 kg in weight. As shown in Fig. 7, these zircon grains are colorless, irregular crystals with long axes varying from 50 μm to 150 μm and length/width ratios from 1.2 to 2.5. CL images show all zircon crystals from the two samples have dark luminescent cores and narrow, bright luminescent rims (Fig. 7c–f). Omphacite and garnet inclusions have been detected in the rim domains by electron probe microanalysis. Dark luminescent cores from sample 4Y04 are unzoned or weakly zoned (Fig. 7a and b), suggesting strong metamictization. The major domains of dark luminescent cores from sample 2C87 display straight and wide oscillatory growth bands (Fig. 7c and d), which, together with the

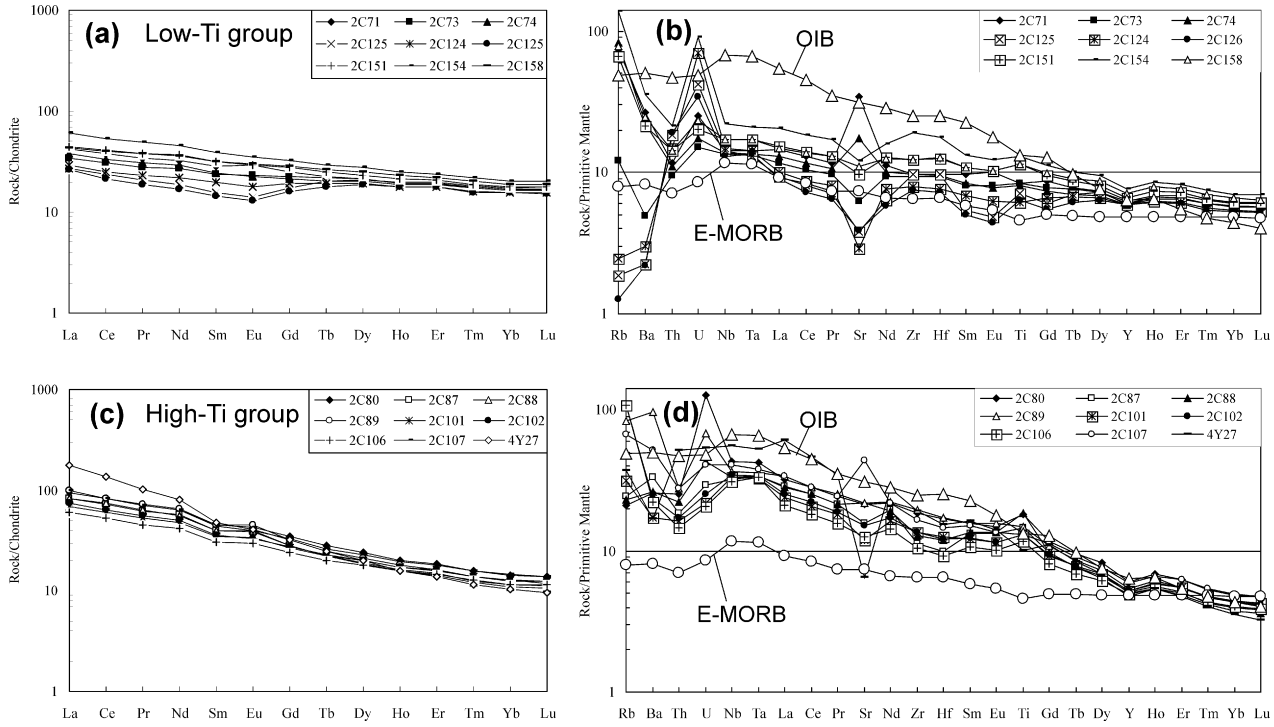

Fig. 6. REE pattern and trace element diagrams of the Yuka eclogites (normalized data from Sun and McDonough (1989).

irregular crystal shape, are interpreted as typical features for zircons from mafic volcanic rocks.

The uranium content in zircons from sample 4Y04 varies in a large range from 184 to 2709 ppm and Th from 153 to 5447 ppm with Th/U ratios of 0.37–4.28. Analyses of 17 zircon grains yield $^{206}Pb/^{238}U$ apparent ages ranging from 439 to 867 Ma and $^{206}Pb/^{207}Pb$ ages from 456 to 848 Ma. However, the metamorphic rims are so thin (<20 μm) that analyses of 18 zircon grains are mostly discordant, and define a mixing line with an upper-intercept age of 847 ± 44 Ma and a lower-intercept age of 433 ± 20 Ma (MSWD = 0.82) in the U–Pb concordia diagram (Fig. 8a).

Twenty-one analyses of 21 zircon cores were obtained for sample 2C87. Uranium content varies from 83 to 650 ppm with Th/U ratios of 0.65–1.49. The apparent $^{206}Pb/^{207}Pb$ ages of the 21 zircon grains range from 804 ± 19 to 882 ± 22 Ma, which are indistinguishable within error, and yield a weighted mean of 847 ± 10 Ma (MSWD = 1.2) (Fig. 8b). In the Tera-Wasserburg Concordia diagrams, an upper intercept age of 848 ± 15 Ma (MSWD = 0.56) was also obtained (Fig. 8b). No metamorphic rims are large enough for analysis.

6. Discussion

6.1. Tectono-petrogenesis of the eclogite protoliths

In the Dulan UHPM terrane, the ophiolitic protoliths (e.g., mantle harzburgite, ultramafic to mafic cumulate, and basaltic rocks) (Song et al., 2003b, 2006; Zhang et al., 2008a,b) give formation ages of 500–550 Ma and HP–UHP metamorphic ages of 460–420 Ma. This points to a tectonic evolution from oceanic lithosphere subduction, to continental collision, to continental lithosphere underthrusting and to the ultimate exhumation (Song et al., 2006, 2009b).

The protoliths of the eclogites from the Yuka terrane, on the other hand, differ significantly from the Dulan ophiolitic sequence. Their occurrence as layers intercalated with terrigenous sedimentary rocks and as dyke-like bodies within the granitic gneisses suggests that the protoliths of these eclogites must be basalts from a continental setting. The high abundances of HFSE and higher Zr/Y and La/Yb ratios are consistent with this interpretation and with their protolith basalts being derived from an enriched mantle source. In primitive mantle normalized trace element diagram (Fig. 6), the high-Ti and low-Ti groups resemble the present-day OIB and E-type MORB, respectively, suggesting the possibility of their mantle plume origin. In the traditional discriminate diagrams (Fig. 9), such as Zr vs. Zr/Y (Pearce and Norry, 1979), Ti vs. V (Shervais, 1982) and Nb–Zr–Y (Meschede, 1986), the LTG eclogites plot in the field transitional between within plate basalts (WPB) and mid-ocean ridge basalts (MORB), but all HTG eclogites plot in the field of WPB. In the La–Y–Nb diagram (Cabanis and Lecolle, 1989) (Fig. 9d), all LTG eclogites plot around the boundary between E-type MORB and continental basalts, and most HTG eclogites fall in the joint regions of continental basalts and alkali basalts from continental rift settings. These geochemical features, together with their host of granitic and pelitic gneisses, suggest that the protoliths of the Yuka eclogite must be basalts from a continental setting, perhaps, genetically associated with a mantle plume in the continental rift stage.

Trace elements in basalts carry the information on their extraction depths or the lithosphere thickness or the amount of extension (McKenzie and O'Nions, 1991; Humphreys and Niu, 2009). The Ce/Yb ratios for LTG eclogites (Ce/Yb = 1.01–9.49) and HTG eclogites (Ce/Yb = 16.34–47.36) suggest that the protoliths of the LTG eclogites may have resulted from melting at a relatively shallow mantle, whereas the protoliths of the HTG eclogites may have derived from melting at a greater mantle depth. This interpretation is consistent with the systematics in Sm/Yb vs. La/Sm plots (Fig. 10), where the HTG protoliths may have a higher proportion of melt produced in the garnet peridotite facies than the LTG protoliths (Humphreys and Niu, 2009).

As discussed above, geochemical features of the Yuka eclogites are best interpreted as a result of mantle plume origin, similar to most continental flood basalts (CFBs) such as the Emeishan CFB in Southwest China (Xu et al., 2001; Xiao et al., 2004), Ethiopian CFB (Pik et al., 1999), northern Karoo CFB (Sweeney et al., 1994), and are

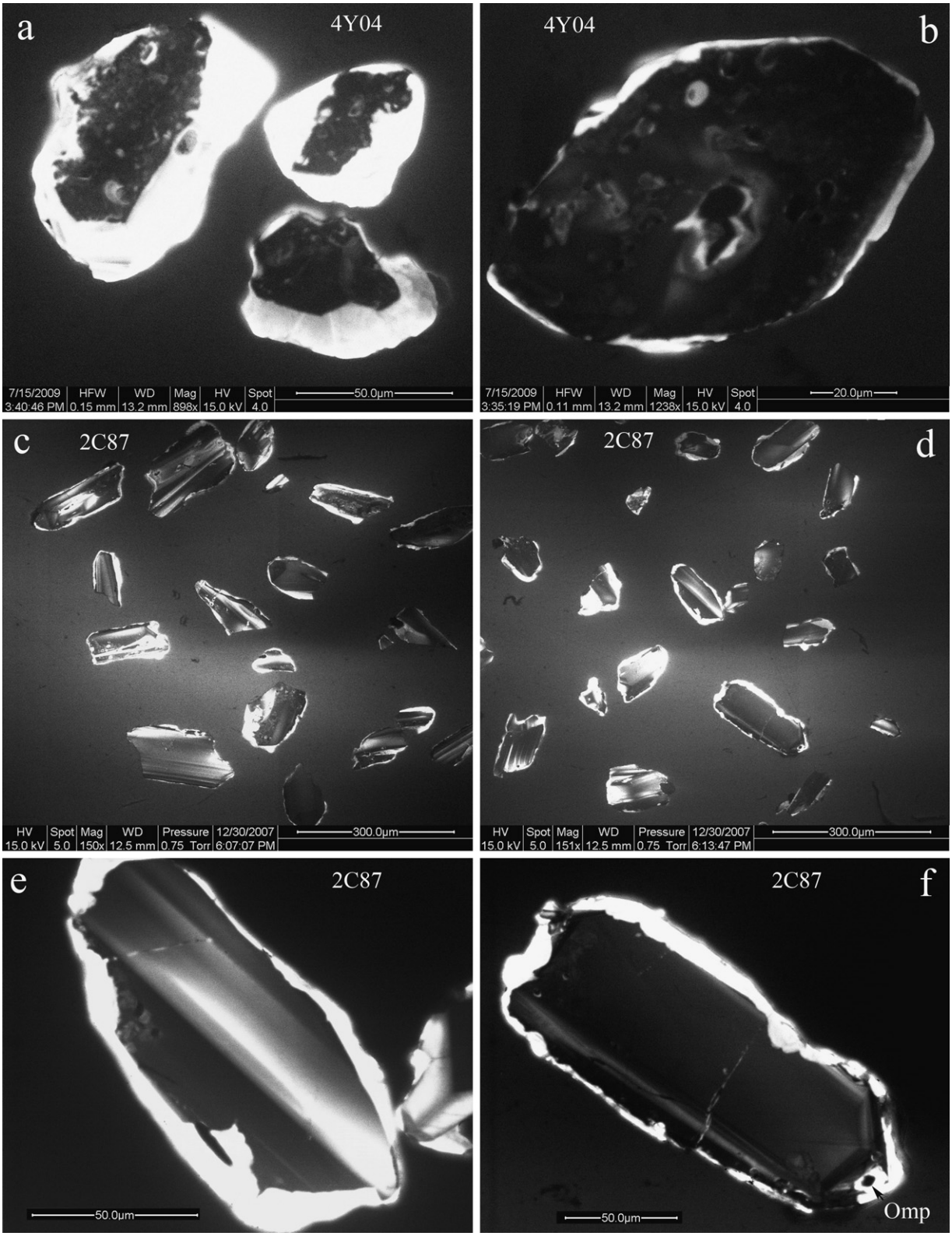

Fig. 7. Cathodoluminescent (CL) images of zircons from Yuka eclogites. (a and b) Relict dark luminescent cores with bright luminescent rims from sample 4Y04; the cores are unzoned and strongly metamictized. (c and d) Irregular zircon crystals showing straight and wide oscillatory growth bands with narrow bright rims (2C87). (e and d) Enlarged images of zircon crystals in (d).

consistent with plume-derived flood basalts as defined by Puffer (2001). For all these reasons, we propose that the protoliths of the Yuka eclogites are continental flood basalts, genetically associated with a mantle plume activity in its early continental rift stage at ~850 Ma.

6.2. Metamorphic and protolith ages of the Yuka eclogites

While it is clear that the Yuka eclogites were formed in response to a continental subduction event in the Early Paleozoic (e.g., Song et al., 2006, 2009b; Mattinson et al., 2007), the exact timing of

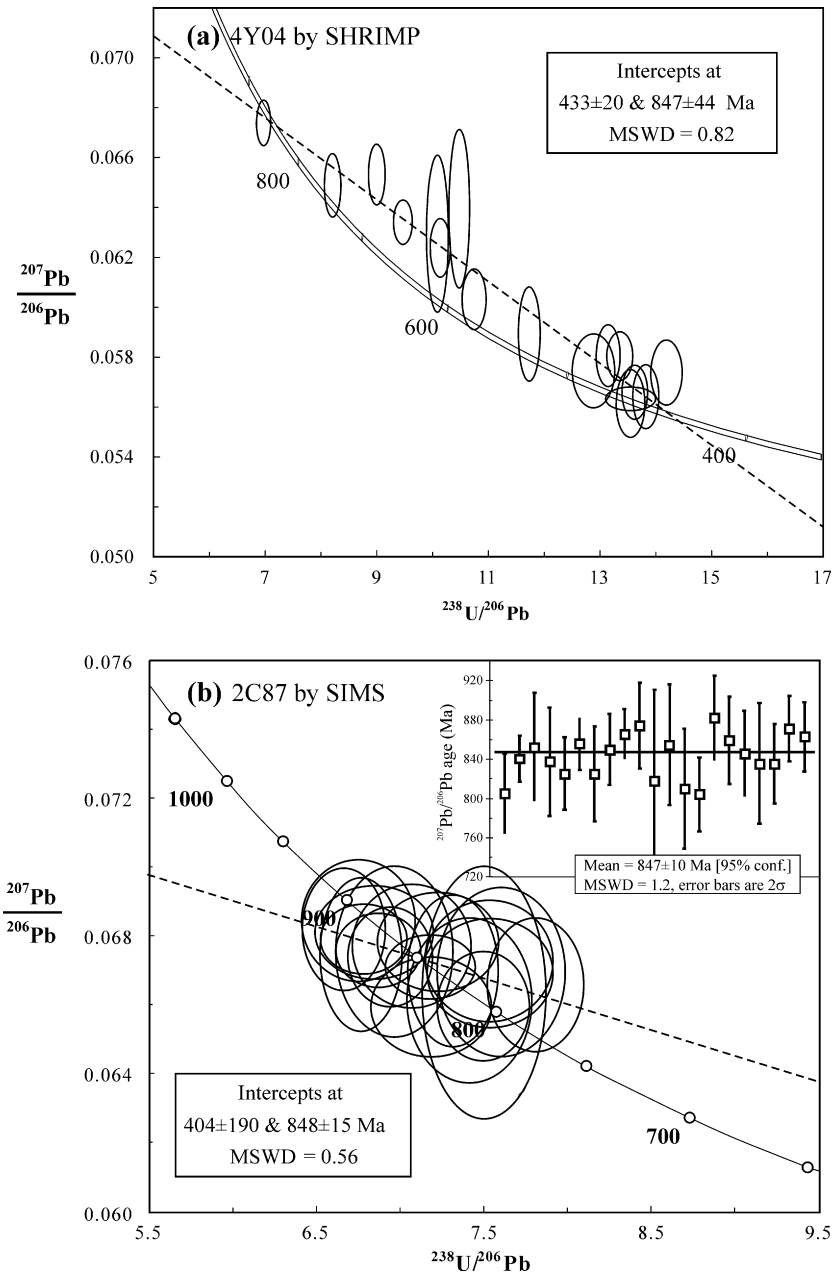

Fig. 8. Tera-Wasserburg (TW) diagrams for zircons from: (a) sample 4Y04 and (b) sample 2C87. All plotted data are corrected using ^{204}Pb and the mean age of 2C87 is ^{207}Pb/^{206}Pb at the 95% confidence level.

this metamorphism has been ambiguous because of analytical difficulties. Using TIMS single zircon U–Pb method, Zhang et al. (2005) suggested the eclogite-facies metamorphism took place at ~500 Ma, but this is likely a "mixing" age because most zircons from the Yuka eclogites have inherited old magmatic cores (vs. metamorphic mantles and rims). Zircons from a metapelite sample yield detrital ^{207}Pb/^{206}Pb ages ranging from 950 to 2216 Ma (Song et al., 2006), and the metamorphic rims are too thin to be analyzed by SHRIMP. Recently, Chen et al. (2009) have obtained eclogite-facies metamorphic (zircon rim) ages of 431 ± 4 Ma and 436 ± 3 Ma for two eclogite samples and of 431 ± 3 Ma and 432 ± 19 Ma for two metapelite samples. They have also given approximate protolith (zircon core) ages of >750 Ma for the eclogite samples.

Zircons in our two eclogite samples show characteristics that are similar to zircons from mafic volcanic rocks. The uniform CL images and U–Pb ages (2C87) suggest that zircons were crystallized from the melt other than crustal assimilation/contamination. In spite of eclogite metamorphism, their metamorphic rims are too thin to be properly analyzed. The upper intercept ages of 848 ± 15 Ma (for both samples) and ^{207}Pb/^{206}Pb mean age of 847 ± 10 Ma should represent the protolith age of the Yuka eclogite and are therefore the formation age of the continental flood basalts as we interpret. Given the fact that only limited samples can give reliable HP metamorphic age in the Yuka eclogite and metapelite samples, we reason that the limited metamorphic growth (thin rims) of zircons suggests a relatively dry condition that disfavors fluid-facilitated diffusion and zircon growth during continental subduction.

6.3. Tectonic implications

The Neoproterozoic (~830–720 Ma) continental intraplate magmatism is widespread on several continents including Australia, Laurentia, South China, South Korea, India, Seychelles and Tarim. This global intraplate magmatism has commonly been attributed to

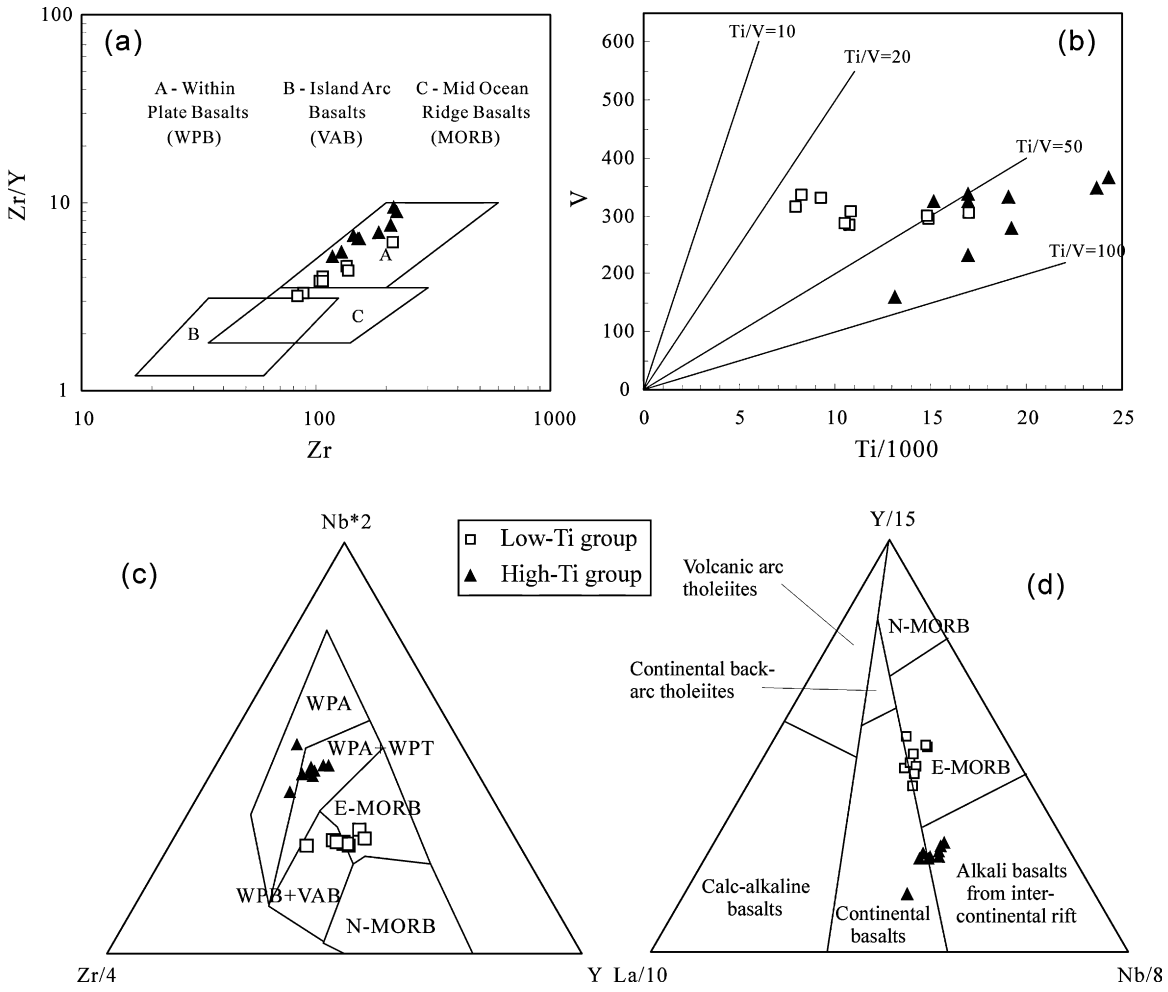

Fig. 9. Discrimination diagrams for the Yuka eclogites: (a) Zr vs. Zr/Y diagram after Pearce and Norry (1979); (b) Ti vs. V diagram after Shervais (1982); (c) Nb–Zr–Y diagram after Meschede (1986); (d) La–Y–Nb diagram after Cabanis and Lecolle (1989).

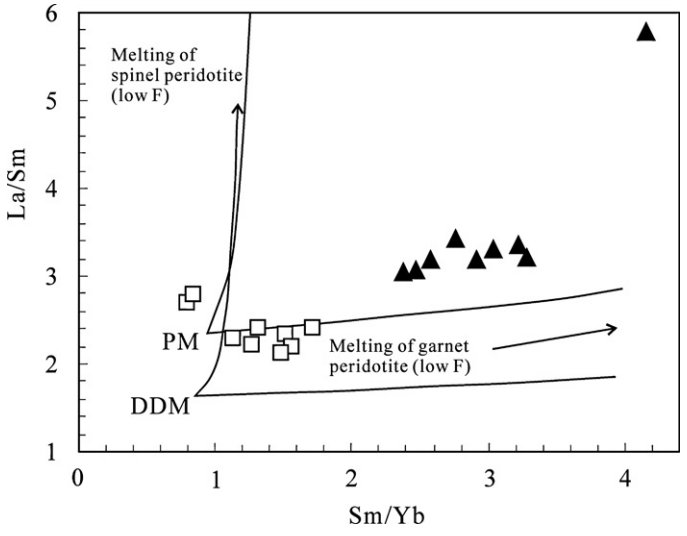

Fig. 10. Sm/Yb vs. La/Sm diagram for the Yuka eclogites. Batch melting trends for garnet and spinel peridotite are after Lassiter and DePaolo (1997). Arrows denote the effect of decreasing melt fraction (F). This plot shows that LTG eclogites underwent higher degree partial melting than that of HTG eclogites. Extremely high La/Sm and Sm/Yb ratios of HTG eclogites suggest that protoliths of HTG eclogites originated from garnet-bearing mantle source, and experienced lower degree partial melting than protoliths of the LTG eclogites.

mantle plumes or a superplume that caused breakup and fragmentation of the supercontinent Rodinia (e.g., Heaman et al., 1992; Zhao et al., 1994; Park et al., 1995; Li et al., 1999, 2003, 2006, 2008a,b; Frimmel et al., 2001; Shellnutt et al., 2004). These Neoproterozoic plume-related igneous rocks include the 850–820 Ma mafic to ultramfic dykes and the 830–740 Ma granite–diabase complex and bimodal (basalt-rhyolite) volcanic rocks in south China (e.g., Li et al., 2003, 2008a,b and references therein). The 825 Ma Yiyang komatiitic basalts in the south China were thought to be generated by melting of an anomalously hot mantle source ($T > 1500\,^{\circ}C$) (Wang et al., 2007). The 830 Ma Jinchuan ultramafic intrusions with Cu–Ni ore deposits and dolerite dykes in northwestern China have also been thought to be of plume origin (Li et al., 2005).

Generally, initial activity of a mantle plume can produce a large quantity of basaltic magmas and forms CFBs or basaltic plateaus. Most researchers suggested that the mantle plume activity that initiated rifting of Rodinia started at ~820 Ma or earlier (e.g., Li et al., 1999). The "global" scale onset of the Neoproterozoic mantle superplume, however, is a matter of debate. This is because most CFBs must have been eroded or destructed during the long history of weathering and fragmentation of the supercontinent. The ~850 Ma Shenwu dolerite dykes reported by Li et al. (2008b) are the earliest intraplate basaltic rocks that may be related to the Rodinia breakup. Zircons from the 825-Ma Yiyang komatiitic basalts also have an age group of 862 ± 6 Ma (Wang et al., 2007), although this age was interpreted as xenocryst zircon age of the magma.

The occurrence and geochemical features of our Yuka eclogite samples suggest that their protoliths are probably of mantle plume origin, similar to most CFBs. The ~850 Ma zircon U–Pb ages may indeed manifest the onset time of large scale plume-related magmatic activities within Rodinia. Therefore, tectonic implications of our new results may be summarized as follows:

(1) The inferred mantle plume that broke up the Rodinia supercontinent may have indeed initiated at ~850 Ma, earlier than 825–830 Ma.
(2) The Qilian-Qaidam blocks represent a composite fragment of Rodinia that has the affinity with the Yangtze craton in the present-day South China.
(3) The evolution history from the breakup (continental rift) to reconstruction (continental subduction and collision) of the supercontinent appears to take a long period of time, ~400 Myrs.

Acknowledgements

We thank Q.L. Li (IGGCAS), T. Ireland (ANU) and X.R. Liang (GIGCAS) for their help with the Lab work. We also thank G.C. Zhao, an anonymous reviewer and Editor P.A. Cawood for their rather constructive review comments, which led to a better presentation of the final product. This study was supported by the Major State Basic Research Development Projects (2009CB825007) and the National Natural Science Foundation of China (Grant Nos. 40825007, 40773012, 40821002, 40802016).

Appendix A. Supplementary data

Supplementary data associated with this article can be found, in the online version, at doi:10.1016/j.precamres.2010.09.008.

References

Cabanis, B., Lecolle, M., 1989. Le diagramme La/10 -Y/15 -Nb/8: Un outil pour la discrimination des series volcaniques et la mise en evidence des procesus de melange et/ou de contamination crutale. Comptes Rendus de l'Académie des Sciences 309, 2023–2029.

Campbell, I.H., Griffiths, R.W., 1990. Implications of mantle plume structure for the evolution of flood basalts. Earth and Planetary Science Letters 99, 79–93.

Chen, D.L., Liu, L., Sun, Y., Liou, J.G., 2009. Geochemistry and zircon U–Pb dating and its implications of the Yukahe HP/UHP terrane, the North Qaidam, NW China. Journal of Asian Earth Sciences 35, 259–272.

Coffin, M.F., Eldholm, O., 1994. Large igneous provinces: crustal structure, dimension, and external consequences. Review of Geophysics 32, 1–36.

Dalziel, I.W.D., Soper, N.J., 2001. Neoproterozoic extension on the Scottish Promontory of Laurentia; paleogeographic and tectonic implications. Journal of Geology 109, 299–317.

Frimmel, H.E., Zartman, R., Späth, E., 2001. The Richtersveld igneous complex, South Africa: U–Pb zircon and geochemical evidence for the beginning of neoproterozoic continental breakup. Journal of Geology 109, 493–508.

Heaman, L.M., LeCheminant, A.N., Rainbird, R.H., 1992. Nature and timing of Franklin igneous events Canada: implications for a Late Proterozoic mantle plume and the breakup of Laurentia. Earth and Planetary Science Letters 109, 117–131.

Humphreys, E.R., Niu, Y.L., 2009. On the composition of ocean island basalts OIB: the effects of lithospheric thickness variation and mantle metasomatism. Lithos 112, 118–136.

Lassiter, J.C., DePaolo, D.J., 1997. Plume/lithosphere interaction in the generation of continental and oceanic flood basalts: chemical and isotopic constraints. In: Mahoney, J.J., Coffin, M.F. (Eds.), Large Igneous Province: Continental, Oceanic, and Planetary Flood Volcanism. American Geophysical Union Geophysical Monography, pp. 335–355, 100.

Li, Z.X., Li, X.H., Kinny, P.D., Wang, J., 1999. The breakup of Rodinia: did it start with a mantle plume beneath South China? Earth and Planetary Science Letters 173, 171–181.

Li, Z.X., Li, X.H., Kinny, P.D., Wang, J., Zhang, S., Zhou, H., 2003. Geochronology of Neoproterozoic syn-rift magmatism in the Yangtze Craton South China and correlations with other continents: evidence for a mantle superplume that broke up Rodinia. Precambrian Research 122, 85–109.

Li, Z.X., Bogdanova, S.V., Collins, A.S., Davidson, A., De Waele, B., Ernst, R.E., Fitzsimons, I.C.W., Fuck, R.A., Gladkochub, D.P., Jacobs, J., Karlstrom, K.E., Lu, S., Natapov, L.M., Pease, V., Pisarevsky, S.A., Thrane, K., Vernikovsky, V., 2008a. Assembly, configuration, and breakup history of Rodinia: a synthesis. Precambrian Research 160, 179–210.

Li, X.H., Li, Z.X., Zhou, H., Liu, Y., Kinny, P.D., 2002. U–Pb zircon geochronology, geochemistry and Nd isotopic study of Neoproterozoic bimodal volcanic rocks in the Kangdian Rift of South China: implications for the initial rifting of Rodinia. Precambrian Research 113, 135–154.

Li, X.H., Liu, D.Y., Sun, M., Li, W.X., Liang, X.R., Liu, Y., 2004. Precise Sm–Nd and U–Pb isotopic dating of the super-giant Shizhuyuan polymetallic deposit and its host granite, Southeast China. Geological Magazine 141, 225–231.

Li, X.H., Su, L., Chung, S.-L., Li, Z.X., Liu, Y., Song, B., Liu, D.Y., 2005. Formation of the Jinchuan ultramafic intrusion and the world's third largest Ni–Cu sulfide deposit: associated with the 825 Ma south China mantle plume? Geochemistry Geophysics Geosystems 6, Q11004, doi:10.1029/2005GC001006.

Li, X.H., Li, Z.X., Wingate, M.T.D., Chung, S.L., Liu, Y., Lin, G.C., Li, W.X., 2006. Geochemistry of the 755 Ma MundineWell dyke swarm, northwestern Australia: part of a Neoproterozoic mantle superplume beneath Rodinia? Precambrian Research 146, 1–15.

Li, X.H., Li, W.X., Li, Z.X., Liu, Y., 2008b. 850–790 Ma bimodal volcanic and intrusive rocks in northern Zhejiang South China: a major episode of continental rift magmatism during the breakup of Rodinia. Lithos 102, 341–357.

Li, X.H., Liu, Y., Li, Q.L., Guo, C.H., Chamberlain, K.R., 2009. Precise determination of Phanerozoic zircon Pb/Pb age by multicollector SIMS without external standardization. Geochemistry Geophysics Geosystems 10, Q04010, doi:10.1029/2009GC002400.

Li, X.H., Li, W.X., Li, Q.L., Wang, X.C., Liu, Y., Yang, Y.H., 2010. Petrogenesis and tectonic significance of the ~850 Ma Gangbian alkaline complex in South China: evidence from in situ zircon U–Pb dating Hf–O isotopes and whole-rock geochemistry. Lithos 114, 1–15.

Lu, S.N., 2002. Preliminary Study of Precambrian Geology in the North Tibet-Qinghai Plateau. Geological Publishing House, Beijing, pp. 1–125 (in Chinese).

Mattinson, C.G., Wooden, J.L., Liou, J.G., Bird, D.K., Wu, C.L., 2006. Age and duration of eclogite-facies metamorphism, North Qaidam HP/UHP terrane, western China. American Journal of Science 306, 683–711.

Mattinson, C.G., Menold, C.A., Zhang, J.X., Bird, D.K., 2007. High- and ultrahigh-pressure metamorphism in the North Qaidam and South Altyn Terranes, western China. International Geology Review 49, 969–995.

Mattinson, C.G., Wooden, J.L., Zhang, J., Bird, D.K., 2009. Paragneiss zircon geochronology and trace element geochemistry, North Qaidam HP/UHP terrane, western China. Journal of Asian Earth Sciences 35, 298–309.

McKenzie, D.P, O'Nions, R.K., 1991. Partial melt distribution from inversion of rare earth element concentrations. Journal of Petrology 32, 1021–1091.

Meschede, M., 1986. A method of discriminating between different types of mid-ocean ridge basalts and continental tholeiites with the Nb–Zr–Y diagram. Chemical Geology 83, 55–69.

Park, J.K., Buchan, K.L., Harlan, S.S., 1995. A proposed giant radiating dyke swarm fragmented by the separation of Laurentia and Australia based on paleomagnetism of ca. 780 Ma mafic intrusions in western North America. Earth and Planetary Science Letters 132, 129–139.

Paulsson, O., Andreasson, P.G., 2002. Attempted break-up of Rodinia at 850 Ma: geochronological evidence from the Seve-Kalak Superterrane Scandinavian Caledonides. Journal of Geological Society 159, 751–761.

Peate, D.W., Hawkesworth, C.J., Mantovani, M.S.M., 1992. Chemical stratigraphy of the Parana lavas, South America: classification of magma-types and their spatial distribution. Bulletin of Volcanology 55, 119–139.

Pearce, J.A., Norry, M.J., 1979. Petrogenetic implications of Ti, Zr, Y and Nb variations in volcanic rocks. Contributions to Mineralogy and Petrology 69, 33–47.

Pik, R., Deniel, C., Coulon, C., Yirgu, G., Marty, B., 1999. Isotopic and trace element signatures of Ethiopian flood basalts: evidence for plume–lithosphere interactions. Geochimica et Cosmochimica Acta 63, 2263–2279.

Puffer, J.H., 2001. Contrasting high field strength element contents of continental flood basalts from plume versus reactivated-arc sources. Geology 29, 675–678.

Richards, M.A., Duncan, R.A., Courtillot, V.E., 1989. Flood basalts and hot-spot tracks: plume heads and tails. Science 246, 103–107.

Rubatto, D., Gebauer, D., Fanning, M., 1998. Jurassic formation and Eocene subduction of the Zermatt-Saas-Fee ophiolites: implications for the geodynamic evolution of the Central and Western Alps. Contributions to Mineralogy and Petrology 132, 269–287.

Shellnutt, J.G., Dostal, J., Keppie, J.D., 2004. Petrogenesis of the 723 Ma Coronation sills, Amundsen basin Arctic Canada: implications for the breakup of Rodinia. Precambrian Research 129, 309–324.

Shervais, J.W., 1982. Ti—V plots and the petrogenesis of modern and ophiolitic lavas. Earth and Planetary Science Letters 59, 101–108.

Song, S.G., Yang, J.S., Xu, Z.Q., Liou, J.G., Wu, C.L., Shi, R.D., 2003a. Metamorphic evolution of coesite-bearing UHP terrane in the North Qaidam, northern Tibet, NW China. Journal of Metamorphic Geology 21, 631–644.

Song, S.G., Yang, J.S., Liou, J.G., Wu, C.L., Shi, R.D., Xu, Z.Q., 2003b. Petrology, Geochemistry and isotopic ages of eclogites in the Dulan UHPM terrane, the North Qaidam, NW China. Lithos 70, 195–211.

Song, S.G., Zhang, L.F., Niu, Y., 2004. Ultra-deep origin of garnet peridotite from the North Qaidam ultrahigh-pressure belt, Northern Tibetan Plateau, NW China. American Mineralogist 89, 1330–1336.

Song, S.G., Zhang, L.F., Niu, Y.L., Su, L., Jian, P., Liu, D.Y., 2005. Geochronology of diamond-bearing zircons from garnet peridotite in the North Qaidam UHPM belt Northern Tibetan Plateau: a record of complex histories from oceanic lithosphere subduction to continental collision. Earth and Planetary Science Letters 234, 99–118.

Song, S.G., Zhang, L.F., Niu, Y.L., Su, L., Song, B., Liu, D.Y., 2006. Evolution from oceanic subduction to continental collision: a case study of the Northern Tibetan Plateau inferred from geochemical and geochronological data. Journal of Petrology 47, 435–455.

Song, S.G., Su, L., Niu, Y.L., Zhang, L.F., 2007. Petrological and Geochemical Constraints on the Origin of Garnet Peridotite in the North Qaidam Ultrahigh-pressure Metamorphic Belt Northwestern China. Lithos 96, 243–265.

Song, S.G., Niu, Y.L., Zhang, L.F., Wei, C.J., Liou, J.G., Su, L., 2009a. Tectonic evolution of Early Paleozoic HP metamorphic rocks in the North Qilian Mountains, NW China: a perspective. Journal of Asian Earth Science 35, 285–297.

Song, S.G., Su, L., Niu, Y.L., Zhang, G.B., Zhang, L.F., 2009b. Two types of peridotite in North Qaidam UHPM belt and their tectonic implications for oceanic and continental subduction: a review. Journal of Asian Earth Science 35, 285–297.

Sun, S.S., McDonough, W.F., 1989. Chemical and isotopic systematics of oceanic basalt: implications for mantle composition and processes. In: Saunders, A.D., Norry, M.J. (Eds.), Magmatism in the Ocean Basins. Special Publications, Geological Society, London, pp. 313–345, 42.

Sweeney, R.J., Duncan, A.R., Erlan, A.J., 1994. Geochemistry and petrogenesis of central Lebombo basalts of the Karoo igneous province. Journal of Petrology 35, 95–125.

Stacey, J.S., Kramers, J.D., 1975. Approximation of terrestrial lead isotope evolution by a two-stage model. Earth and Planetary Science Letters 26, 207–221.

Wan, Y.S., Xu, Z.Q., Yan, J.S., Zhang, J.X., 2001. Ages and compositions of the Precambrian high-grade basement of the Qilian Terrane and its adjacent areas. Acta Geologica Sinica 75, 375–384.

Wang, X.C., Li, X.H., Li, W.X., Li, Z.X., 2007. Ca 825 Ma komatiitic basalts in South China: first evidence for >1500 °C mantle melts by a Rodinian mantle plume. Geology 35, 1103–1106.

Wang, X.C., Li, X.H., Li, W.X., Li, Z.X., Liu, Y., Yang, Y.H., Liang, X.R., Tu, X.L., 2008. The Bikou basalts in northwestern Yangtze Block South China: remnants of 820–810 Ma continental flood basalts? GSA Bulletin 120, 1478–1492.

Wiedenbeck, M., Alle, P., Corfu, F., Griffin, W.L., Meier, M., Oberli, F., Vonquadt, A., Roddick, J.C., Speigel, W., 1995. Three natural zircon standards for U–Th–Pb Lu–Hf, trace-element and REE analyses. Geostandard Newsletters 19, 1–23.

Winchester, J.A., Floyd, P.A., 1977. Geochemical discrimination of different magma series and their differentiation products using immobile elements. Geochemical Geology 20, 325–343.

White, R.S., McKenzie, D.P., 1989. Magmatism at rift zones: the generation of volcanic continental margins and flood basalts. Journal of Geophysics Research 94, 7730–7685.

Yang, J.S., Xu, Z.Q., Li, H.B., Wu, C.L., Cui, J.W., Zhang, J.X., Chen, W., 1998. Discovery of eclogite at northern margin of Qaidam basin NW China. Chinese Science Bulletin 43, 1755–1760.

Yang, J.S., Xu, Z.Q., Song, S.G., Zhang, J., Wu, C., Shi, R., Li, H., Brunel, M., 2001. Discovery of coesite in the North Qaidam Early Palaeozoic ultrahigh pressure, UHP metamorphic belt NW China. Comptes Rendus De L Academie Des Sciences Serie II Fascicule A-Sciences De La Terre et Des Planetes 11, 719–724, 333.

Yang, J.S., Xu, Z.Q., Song, S.G., Zhang, J.X., Wu, C.L., Shi, R.D., Li, H.B., Brunel, M., Tapponnier, P., 2002. Subduction of continental crust in the early Paleozoic North Qaidam ultrahigh-pressure metamorphism belt NW China: evidence from the discovery of coesite in the belt. Acta Geologica Sinica 76, 63–68.

Yang, J.S., Wu, C.L., Zhang, J.X., Shi, R.D., Meng, F.C., Wooden, J., Yang, H.Y., 2006. Protolith of eclogites in the north Qaidam and Altun UHP terrane NW China: earlier oceanic crust? Journal of Asian Earth Sciences 28, 185–204.

Xiao, L., Xu, Y.G., Mei, H.J., Zheng, Y.F., He, B., Pirajno, F., 2004. Distinct mantle sources of low-Ti and high-Ti basalts from the western Emeishan large igneous province SW China: implications for plume–lithosphere interaction. Earth and Planetary Science Letters 228, 525–546.

Xu, Y.G., Chung, S.L., Jahn, B.M., Wu, G.Y., 2001. Petrologic and geochemical constraints on the petrogenesis of Permian–Triassic Emeishan flood basalts in southwestern China. Lithos 58, 145–168.

Zhang, G.B., Song, S.G., Zhang, L.F., Niu, Y.L., 2008a. The subducted oceanic crust within continental-type UHP metamorphic belt in the North Qaidam NW China: evidence from petrology, geochemistry and geochronology. Lithos 104, 99–108.

Zhang, G.B., Zhang, L.F., Song, S.G., Niu, Y.L., 2009a. UHP metamorphic evolution and SHRIMP dating of meta-ophiolitic gabbro in the North Qaidam, NW China. Journal of Asian Earth Sciences 35, 310–322.

Zhang, G.B., Ellis, D.J., Christy, A.G., Zhang, L.F., Niu, Y.L., Song, S.G., 2009b. UHP metamorphic evolution of coesite-bearing eclogite from the Yuka terrane, North Qaidam UHPM belt, NW China. European Journal of Mineralogy 21, 1287–1300.

Zhang, J.X., Yang, J.S., Mattinson, C.G., Xu, Z.Q., Meng, F.C., Shi, R.D., 2005. Two contrasting eclogite cooling histories North Qaidam HP/UHP terrane, western China: petrological and isotopic constraints. Lithos 84, 51–76.

Zhang, J.X., Mattinson, C.G., Meng, F., Wan, Y., Dong, K., 2008b. Polyphase tectonothermal history recorded in granulitized gneisses from the North Qaidam HP/UHP metamorphic terrane Western China: evidence from zircon U–Pb geochronology. Geological Society of America Bulletin 120, 732–749.

Zhao, J.X., McCulloch, M.T., Korsch, R.J., 1994. Characterisation of a plume-related ~800 Ma magmatic event and its implications for basin formation in central-southern Australia. Earth and Planetary Science Letters 121, 349–367.